Measuring Americium and Cesium Gamma Ray Energy Losses Caused by Compton Scattering through Al and Pb Targets

Denisse Córdova Carrizales, Yao Yin[1, *]

[1]*Department of Physics, Harvard University, Cambridge, Massachusetts 02138, USA*
(Dated: October 14, 2021)

Abstract: In this scattering experiment, we use ^{137}Cs and ^{241}Am as gamma radiation sources, lead and aluminum as scattering targets, and a NaI(Tl) scintillator and a germanium detector to probe the theory of electromagnetic radiation as a quantum phenomena. We compare our scattering energy losses to the predicted values of Compton's scattering energy loss derivation and compare our scattering cross section to the Klein-Nishina formula. The energy losses predicted by Compton agree with our data within one standard deviation, except for the scattering americium by lead. ~~Finding the absolute cross section in scattering experiments is a rare feat, and the absolute values of our scattering cross section calculations do not agree with Klein-Nishina's predictions. However, the functional form of the scattering cross sections of both sources scattered by lead agree within one standard deviation.~~ We conclude that our data does indeed support the theory that the scattering of gamma radiation is a quantum phenomena.

I. INTRODUCTION

In 1923, Arthur Holly Compton studied the loss of energy and, consequently, the lengthening wavelength of x-rays scattered at different angles. Notably, Compton observed that the loss of energy is independent of scattering targets, dependent only on the rays' scattering angle. Compton's observations were in stark disagreement with Sir Joseph John Thompson's 1907 theory of elastic scattering of electromagnetic radiation by a free electron. In Thompson's theory, the outgoing, scattered wave carries the exact same energy and frequency as the incident wave. Compton's observations, later coined the Compton effect, were some of the first validations of quantum theory, asserting electromagnetic radiation is both a wave and a particle[1]. In this paper, we recreate Compton's experiment using gamma rays instead of x-rays and use our data to further support the wave-particle duality.

More specifically, we measure the energy losses of ^{137}Cs (662 keV) and ^{241}Am (59.6 keV) gamma radiation scattered by aluminum and lead targets. We use two different radiation sources and two types of scattering targets in order to probe the variables that affect 1) the collected radiation intensity, 2) the shape and intensity of the Compton shift, 3) the broadening of the Compton peak, and 4) the validity of impulse approximation (see Section II). We compare our energy loss observations to the theoretical values derived from the Compton energy equation 2. We also calculate the differential cross sections for each scattering target and radiation source and compare our results to the theoretical predictions by the Klein–Nishina formula 7, a derivation meant to more accurately describe the scattering of electromagnetic radiation by taking Compton scattering into account than the cross section formula informed by Thompson scattering which is accurate only for low-energy electromagnetic radiation.

In Section II, we present brief derivations and explanations of the theoretical equations proposed by Compton and Klein-Nishina, as well as the theoretical framework of our apparatus. In Section III, we detail the experimental procedures. In Section IV, we present our results, compare them to theoretical values, and discuss any error considerations.

II. THEORY

~~In equation 1, we will derive that the wavelength shift for any incident radiation is independent of the wavelength of the incident ray and dependent only on the angle of the incident ray. Therefore, for low-energy radiation, the wavelength shift is a small fraction of the incident wavelength and, consequently, more difficult to detect. The wavelength shift in high-energy radiation, which is the same magnitude as the wavelength shift in low-energy radiation, is therefore a larger fraction of the incident wavelength, making it easier to detect. We used gamma radiation in this experiment since it has more easily detectable wavelength shift which is easier for us to detect than the x-radiation shift compared to x-ray.~~

A. Compton Scattering

Compton's scattering theory begins with the important assumption that electrons in the scattering target can be approximated as free but stationary prior to any collisions with photons. This *impulse approximation* is possible only if the incident ray energy is much larger than the electrons' binding energies of the scattering targets[2]. Therefore, at lower incident energies, impulse approximation fails.

When an incident ray hits a target, it is scattered by a single electron on the outer most shell of an atom in the target. The scattered ray leaves the target with a lower energy than the incident ray. To conserve momentum of the system, the target electron recoils.

We can treat the incident ray as a particle in the form of a photon. Using conservation of energy and momentum, we can calculate the wavelength of the scattered rays as a function of incident angle[1]:

$$\lambda_\theta = \lambda_0 + \frac{2h}{mc}\sin^2(\frac{1}{2}\theta) = \lambda_0(1-\cos\theta) \qquad (1)$$

where m is the mass of the electron, h is the plank constant, and c is the speed of light. The constant $\frac{h}{mc}$ is the Compton wavelength of the recoiled electron and has the value 2.42×10^{-13}m. We can rewrite equation 1 in terms of energy, using $E = \frac{hc}{\lambda}$:

$$E_\theta = \frac{E}{1 + \frac{E}{mc^2}(1-\cos\theta)} \qquad (2)$$

Where E is the incident ray energy and E_θ is the scattered ray energy[1].

We can further investigate the properties of the scattering event by looking at the scattering cross section of a single incident photon by a single target electron:

$$\sigma = \frac{\text{scattered flux}}{\text{incident flux per unit area}} \qquad (3)$$

The differential cross section of a single scatter is thus defined as:

$$\frac{d\sigma}{d\Omega} = \frac{\text{scattered flux at differential angle}}{\text{incident flux per unit area}} \qquad (4)$$

and has units of cm^2/sr in this paper.

Before Compton's discovery, Thompson's classical scattering theory was used to derive the differential scattering cross section where r_0 is the classical electron radius and θ is the scattering angle[3]

$$\frac{d\sigma}{d\Omega_T} = r_0^2 \frac{1+cos(\theta)^2}{2} \qquad (5)$$

which when integrated over all angles results in the Thompson cross section[3]

$$\sigma_T = \frac{8\pi}{3}r_0^2 \qquad (6)$$

Thompson's derivations were used widely to calculate the cross sections of high energy incident rays, and it was shown to be highly inaccurate[4].

Following Compton's discovery of quantum mechanical radiation scattering, Oskar Klein and Yoshio Nishina derived the Klein-Nishina formula to more accurately describe the energy losses of incident ray and target electron collisions and predict the cross sections of scattering experiments[3]:

$$\frac{d\sigma}{d\Omega} = (\frac{1}{2}\frac{e^2}{mc^2})^2 f(E_\gamma,\theta)(f(E_\gamma,\theta) + f(E_\gamma,\theta)^{-1} - \sin^2\theta) \qquad (7)$$

where $f(E_\gamma,\theta)$ is the ratio between the scattered photon energy and the incident photon energy, or $\frac{E_{theta}}{E_0} = \frac{1}{1+\frac{E}{mc^2}(1-\cos\theta)}$, directly using Compton's formula.

Experimentally, the cross section can be calculated by examining the intensities of the shifted Compton peaks, integrating the total counts of the peak, and accounting for integration time. For detailed treatment of data, see section IV.

B. Sodium Iodide Gamma Ray Detectors

Scintillators produce photons when ionizing radiation interacts with their luminescent crystal. The crystal is usually NaI, and it is paired with a photomultiplier tube (PMT). Scintillation counters detect high energy radiation and convert its energy to a readable electronic signal. When radiation strikes the crystal, a flash of light is produced and strikes the photo multiplier tube, which then amplifies the signal of the photons and converts them into electrons via the photoelectric process. The PMT requires a high voltage power supply to accelerate electrons onto dynodes in order to multiply them. The pulse that comes from the PMT has an amplitude of millivolts, and it is amplified by a pre-amp and then an amplifier to the scale of a volt, which then allows us to visualize the pulse from the PMT on an oscilloscope and capture the voltage distributions using a pulse height analyzer (PHA). It is crucial to note that the intensity of the light produced by the scintillation crystal is proportional to the energy of the incident radiation, thus we can use such a device to measure the voltage spectrum of a certain material. A detailed view of the signal chain in plotted in 1.

C. Germanium Gamma Ray Detectors

Solid state detectors consist of parallel plate capacitors with a semiconducting dieletric, like germanium, and incoming gamma radiation ionizes atoms in the dielectric, creating electron-hole pairs[5]. Excited electrons move toward the anode and holes move toward the cathode, charging the capacitor. The magnitude of the voltage is proportional to the energy of the radiation. The resolution of solid state detectors depends on the energy band gap of the dielectric, so germanium detectors are preferred over silicon detectors[5]. And, in general, germanium detectors have a finer resolution than NaI scintillators.[5]. However, germanium's small band gap makes detectors at room temperature prone to leakage current caused by the flow of electrons thermal excitations, so germanium detectors must be cooled to 77K[5].

The voltage between the capacitor plates is amplified by a pre-amp and then an amplifier to the scale of a volt, which then allows us to visualize the pulse from the PMT on an oscilloscope and capture the voltage distributions using a pulse height analyzer (PHA). A detailed view of the signal chain in plotted in 1.

III.   APPARATUS AND METHODS

At low incident energies, the Compton energy shift is relatively small, so we used a germanium detector that has a higher energy resolution than a NaI(Tl) scintillator to collect the radiation of [241]Am (59.6 keV). While the germanium detector is ∼ 100 efficien 60 keV, its efficiency drops exponentially at higher energies. For this reason, and to be able to confirm the Compton effect on different detectors, we used a NaI(Tl) scintillator to collect the radiation of ^{137}Cs (662 keV) (See Section II B for details and **??** for specifications of our setup). The NaI detector is also used for the confirmation of Compton scattering due to its large absorption cross section as a result of iodine's large atomic number.[5]

In between the radiation source and the detectors, we placed a cylindrical aluminum scattering target (diameter = 1.9 cm) and a cylindrical lead scattering target (diameter = 1.9 cm) in sequence.

The thickness of the Al and Pb is negligible since the λ = 4.7 cm in Al and λ = .92 cm in Pb λ = 1.3 cm in Al[6] and λ = .02 cm in Pb[7] for ^{241}Am. when we used a plate we made sure to bisect the angle of the gamma rays coming in to minimize the matter it interacted with.

Furthermore, the mean free path λ of gamma rays in air is 10^4 cm[3], and the mean free path of ^{241}Am gamma rays in air is 10^3 cm[7]. The total distance in air that either isotope's gamma rays traveled from the source to the respective detector was 35.5 cm, so the interaction of gamma rays in the air is negligible.

The range of a recoil electron scattered by ^{137}Cs in Al is .06 cm[3]. Given that Pb has a higher Z, the range of a recoil electron scattered by ^{137}Cs in Pb must be shorter than .06 cm. Furthermore, since the Compton wavelength for an electron is independent of incident angle or energy, recoil electrons in Al scattered by^{241}Am have a range of .06 cm. Given that Pb has a higher Z, the range of a recoil electron scattered by ^{241}Am in Pb must be shorter than .06 cm. This means that recoil electrons almost always stop in the scattering target and are not detected by either detector.

Systematic errors that arose during our data collection include: 1) We did not recalibrate the binning of our data before and after every time that we collected our data. Subtle drifts could have arisen without us noticing. In fact, during the last collection of our data of americium scattering off of lead, we did notice a drift in our gain that shifted all of the collected peak noticeably out of line. So we recollected calibration data. However, this was the only time this was done. 2) The energy resolution of NaI detectors is visibly worse than the resolution of germanium detectors.
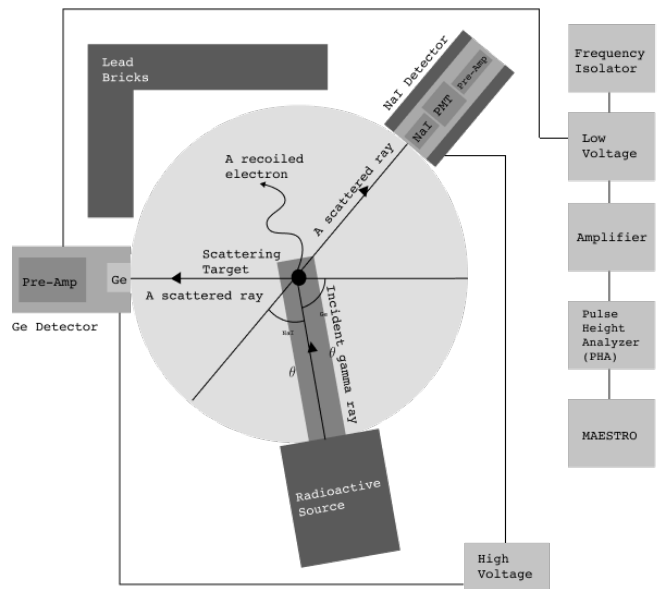

FIG. 1: Compton Scattering of Gamma Rays Experimental Setup: 0° is defined as the detector pointing directly at the respective detector. ^{137}Cs and ^{241}Am were placed in the collimator one after the other. The recoiled electron path is not drawn to scale.

IV.   DATA ANALYSIS AND DISCUSSION

A.   Scattering of Cesium Gamma Rays Using Sodium Iodide Doped with Thallium Detector

Importantly, NaI doped with thallium has an increased luminesence at room temperature[5], so we used a detector with a NaI crystal doped with thallium. We calibrated our NaI(Tl) scintillator by placing ^{133}Ba, ^{241}Am, ^{22}Na, ^{137}Cs, and ^{60}Co radioactive sources directly in front of the detector and comparing the observed peaks with their known energy peaks, respectively 81 keV and 356 keV; 59.5 keV; 511 keV and 1274 keV; 662 keV; 1173 keV and 1332 keV. To find the values of the observed peaks, we applied a Gaussian fit to each of the desired peaks in the spectra. Then, we found the linear relationship between the observed peak energies and the known energies to calibrate the bin values on the x axis of the MAESTRO software to their respective physical values.

We then observed the behavior of cesium gamma rays over a range of angles from 0° to 150° in varying intervals of 5° and 20°. The energy spectra at 0°, 5°, 10°, and 15° were collected for 120 seconds. The energy spectra at 20°, 25°, 30°, and 50° were collected for 300 seconds. The energy spectra at 90°, 110°, 130°, and 150° were collected for 840 seconds. The signal-to-noise ratio for our data was greater than 5. An example ^{137}Cs energy spectrum is shown in figure 4.

We collected background radiation for 120 seconds. We then selected the Compton peaks (characterized by their shifting energy with the incident angle) from each background-subtracted spectrum and fitted normal
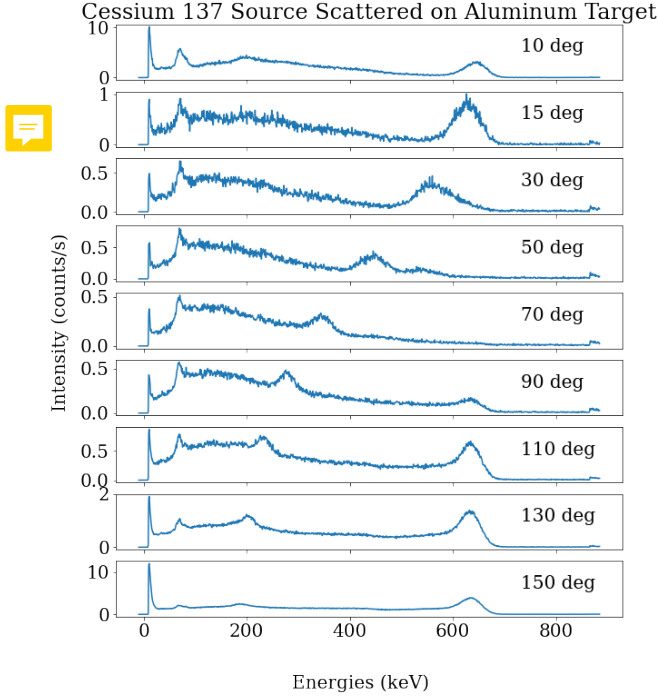
Gaussian profiles to each peak.

Cessium 137 Source Scattered on Aluminum Target

FIG. 2: Raw spectra of Cesium 137 scattered on Aluminum target at different angles. The spectra are not background subtracted but are scaled according to their integration times. When the radiation source is aimed directly at the NaI(Tl) detector ($0°$), an energy peak is centered around ^{137}Cs's expected energy value. As the angle increases, radiation is collected that has lost energy due to collisions with electrons. The shifting energy peak is the Compton peak. Energy peaks observed at 662 keV are from radiation that did not collide with electrons while traveling through the scattering target. Results from other source-target combinations are shown in the appendix.

B. Scattering of Americium Gamma Rays Using Germanium Detector

We calibrated our germanium detector by placing an Americium 241 source directly in front of the detector and comparing the observed peaks with the known Americium energy peaks at 26.3 and 59.5 keV, as well as the Neptunian 237 energy peak at 17.6 keV, which is an alpha decay product of Americium 241. We applied a Gaussian fit to the spectra peaks and found the linear relationship between the observed peak energies and the known energies, in order to calibrate the bin values on the x axis of the MAESTRO software to their respective physical values.

We then observed the behavior of Americium gamma rays over angles ranging from 30° to 150°, with 20° intervals. Due to the weakness of the source, each spectrum

was integrated for 65,000 seconds to get signal-to-noise ratios 10. An example resulting spectrum is shown in figure 4. Due to the lack of background radiation data for an adequate time frame, we used the average value of the spectrum between 30 and 40 keV as a constant background value. We then selected the compton peaks from each background-subtracted spectrum and fitted normal Gaussian profiles to each peak and obtained the mean, amplitude, and standard deviations.
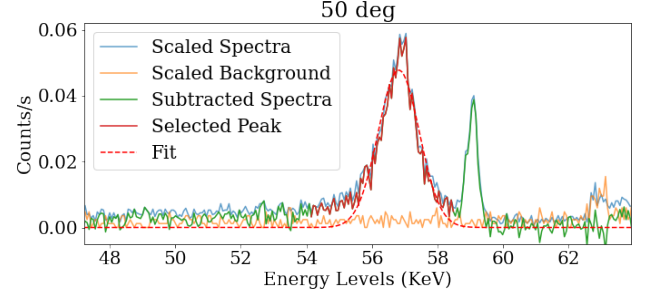

FIG. 3: ^{241}Am scattered by aluminum at $30°$. The Compton peak is in red and labels indicating the elastic peak at 59.5 keV can be seen in green to the right. The Gaussian is highlighted by the red dash line.
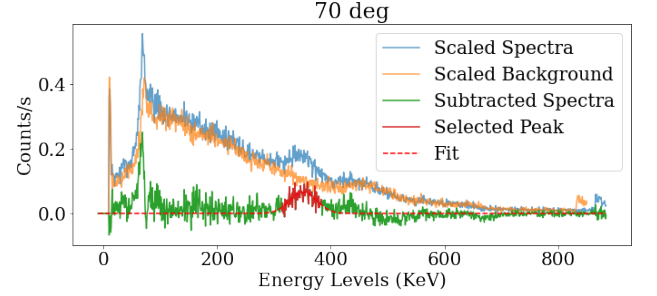

FIG. 4: ^{137}Cs scattered by Lead at a 70°. The Compton peak is in red. The Gaussian is highlighted by the red dash line.

C. Compton Shifts

To obtain the Compton energy curves, we plotted the mean values of the Gaussian fits against their corresponding angles in Figure 5 and compared the observed data with the theoretical predictions according to Equation 2, which is a function of the scattering angle θ and the incident peak energy E_0 only. When we rewrite 2 as and plot $1 - \cos \theta$ against $\frac{1}{E_\theta}$, the corresponding curve should be linear with an offset of $\frac{1}{E_0}$ (662 keV for ^{Cs}137 and 59.5 keV for ^{Am}241) and a slope of $\frac{1}{mc^2}$, where m is the rest mass of an electron. This result is reflected in figures 5 for all combinations of the sources and the scattering targets.

It is interesting to observe that compared to the other combinations, ^{Am}241 scattering upon lead deviated the

most from the theoretical predictions of Compton. This can be explained by the failure of the impulse approximation for high-Z scatterisignal-tng materials. For Al, the k-shell electrons has a binding energy of about 1.56 keV, significantly less than the gamma ray energies of both $^{Am}241$ (59.5 keV) and $^{Cs}137$ (662 keV). However, he k-shell electrons of Pb has a binding energy of 88 keV, significantly less than the gamma ray energies of Americium 241 (59.5 keV). As mentioned in Section II, when the binding energy of the electrons in the scattering target is more than or similar to the energy of the gamma rays, the assumption that Compton made about the electrons being free is no longer entirely valid. The impulse approximation predicts a higher energy from the scattered photon than what is actually observed, due to the fact that more energies are absorbed by the atom in this case to counteract the binding energy of the high-Z scattering target, resulting in a lower energy of the scattered beam.

D. Differential Cross Sections

As mentioned in Section II, the differential cross section quantifies the ratio of the energy of the scattered beam over the energy of the incident beam, in units of area per scattered angle. To obtain the theoretical values of the differential cross section predicted by the Klein-Nishina formula (Equation 7. We can also obtain the theoretical values using the observed Compton shifts, and use $f(E_\gamma, \theta) = \frac{E_\theta}{E_0}$. Predicted results from the two methods are shown in Figure 6, with the values calculated using Compton energy shifts lying consistent with the curve, which is expected due to our data being consistent with the Compton equation (See IV C).

In order to measure the observed differential cross sections from the spectra, we plotted the amplitudes of the Gaussian fits against their corresponding angles, as shown in Figure 6. Since we did not obtain data on the incident gamma ray without any scattering targets, due to the lack of appropriate apparatus, we are not able to obtain the exact ration between the scattered ray and the incident ray, which is required for the calculation of the differential cross section with the correct scaling factors from experimental data. Therefore, the shapes of the curves instead of the actual values are of upmost importance in the plots in Figure 6. As seen from the figures, especially that of the theoretical predictions, the higher the energy levels, the more the shapes of the cross section deviated from the shapes of Thompson scattering and takes more of an exponential form.

V. CONCLUSION

The scattering data collected from both the germanium and NaI(Tl) detectors is accurately predicted by Compton's derivations of scattering energy losses 2 and explained by the transfer of energy of an incident ray to a single target electron. From the agreement of our experiment to the theoretical expectations, we can conclude that the scattering of gamma rays is a quantum phenomena that can be predicted the Compton energy formula and the Klein-Nishina scattering cross-section formula.

VI. COLLABORATION STATEMENT

The authors worked jointly on data collection, analysis, and writing of this paper.
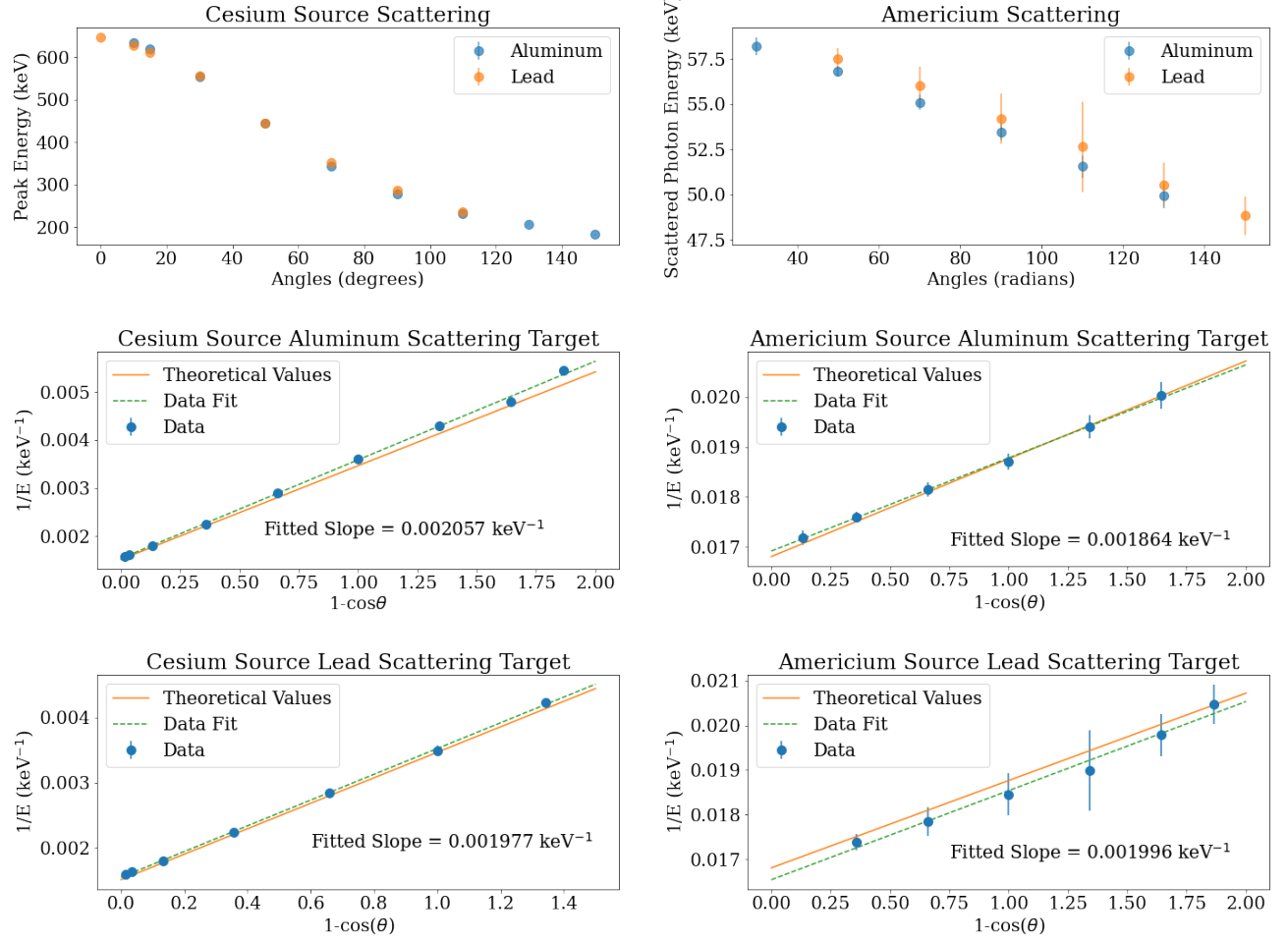
VII. ACKNOWLEDGEMENTS

FIG. 5: Compton shift observed using Americium and Cesium sources with Lead and Aluminum scattering targets. The blue data points are the peak energy values of the selected Compton Peaks with error bars calculated using the covariance matrix of the Gaussian fit, although some error bars are not visible directly on the graph due to the small magnitude. The orange lines are the theoretical energy shifts as a function of angle calculated using Equation 2 and the dashed lines are the linear best fits to the data points. The slope of the fitted linear lines are annotated on the plots. They agree with $\frac{1}{mc^2}$, where m is the rest mass of an electron.
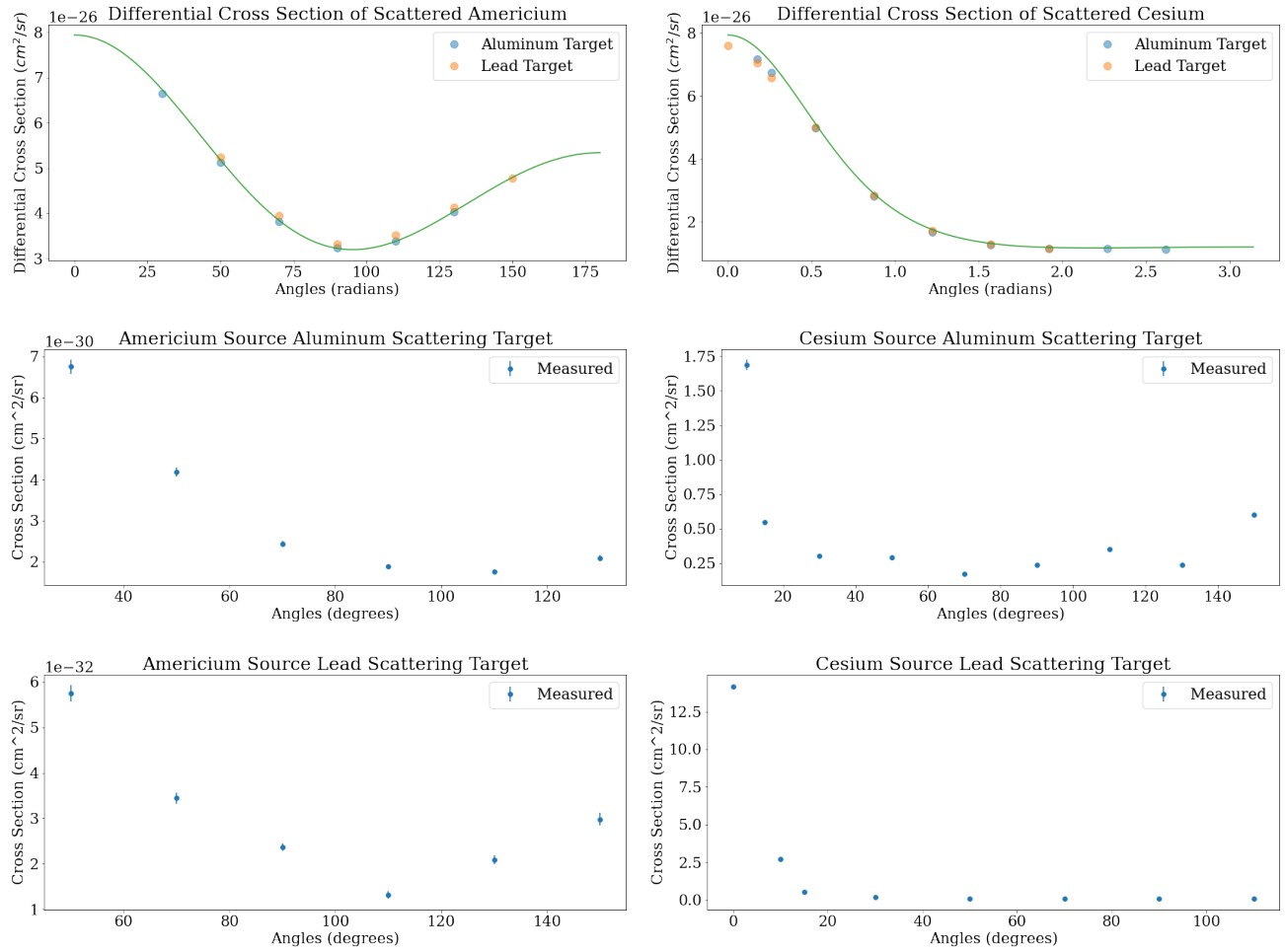
FIG. 6: Scattering cross section of Aluminum source with Lead and Aluminum scattering targets. The top graph plots the theoretical values predicted using the Klein-Nishina formula. The green line is calculated only using the incident photon energy and the colored dots are calculated using the energy ratio of the incident and scattered photon. The middle and bottom plots show the observed cross section calculated using the amplitude of the fitted normal Gaussian to the spectra.

* denissecordovacarrizales@college.harvard.edu;
yyin@college.harvard.edu

[1] Arthur H Compton, "A Quantum Theory of the Scattering of X-rays by Light Elements," Physical Review **21** (1923), 10.1103/PhysRev.21.483.

[2] M J Cooper, "Compton scattering and electron momentum determination," (1985).

[3] Adrian C Melissinos and Fay Ajzenberg-Selove, " Experiments in Modern Physics ," Physics Today **20** (1967), 10.1063/1.3034195.

[4] Albert Allen Bartlett, "Compton Effect: Historical Background," American Journal of Physics **32** (1964), 10.1119/1.1970139.

[5] R.A. Dunlap, *Experimental Physics Modern Methods* (1988) pp. 296–322.

[6] Burcu Akça and Salih Z. Erzeneoğlu, "The Mass Attenuation Coefficients, Electronic, Atomic, and Molecular Cross Sections, Effective Atomic Numbers, and Electron Densities for Compounds of Some Biomedically Important Elements at 59.5keV," Science and Technology of Nuclear Installations **2014** (2014), 10.1155/2014/901465.

[7] J.H. Hubbell and S.M. Seltzer, "Tables of X-Ray Mass Attenuation Coefficients and Mass Energy-Absorption Coefficients from 1 keV to 20 MeV for Elements $Z = 1$ to 92 and 48 Additional Substances of Dosimetric Interest*," NIST Standard Reference Database 126 (2004).